Journal of Carcinogenesis
Covering Genesis to Therapeutics
Journal of Carcinogenesis, ISSN: 1477-3163
2025; Vol24: Issue 10s, https://carcinogenesis.com/

MRI-Based Characterization of Edema-Like Marrow Signal Intensity: A Prospective Case Series of 122 Patients

Dr. Sanjay M. Khaladkar[1], Dr. Neeha Amit Jhala[2*], Dr. Karishma Santosh Krishnani[3], Dr.Eshan Chetan Durgi[4]

[1]Professor, Dr. D.Y. Patil Medical college and hospital and Research centre, Pimpri, Pune – 411018

[2]Resident - Dr. D.Y. Patil Medical college and hospital and Research centre, Pimpri, Pune – 411018

[3]Resident - Dr. D.Y. Patil Medical college and hospital and Research centre, Pimpri, Pune – 411018

[4]Resident - Dr. D.Y. Patil Medical college and hospital and Research centre, Pimpri, Pune – 411018

ABSTRACT

Background: Edema-like marrow signal intensity (ELMSI), earlier referred to as bone marrow edema (BME), is a frequent but nonspecific finding on magnetic resonance imaging (MRI). The AJR consensus panel in 2019 recommended the updated terminology "ELMSI" to reflect its imaging-based nature. Despite this, most published studies continue to use the older term "BME."

Aim: To prospectively evaluate the distribution, imaging patterns, and clinicopathological correlation of ELMSI across different anatomical sites using MRI. To the best of our knowledge, no original study has systematically assessed ELMSI across multiple skeletal regions till date.

Materials and Methods: This prospective observational study included 122 consecutive patients who underwent MRI for suspected marrow pathology between August 2022 and July 2024 at a tertiary care center. MRI was performed on a 3T scanner using T1WI, T2WI, STIR, PDFS, DWI with ADC mapping, and post-contrast sequences when indicated. Patients with physiological marrow changes were excluded. Data on demographics, location, pattern (focal or diffuse), associated features, and final diagnosis were analyzed.

Results: The spine was the most common site of ELMSI (32 cases, 26.2%), followed by the knee (21, 17.2%) and ankle (17, 13.9%). Mean patient age ranged from 39 years (shoulder) to 53 years (knee and wrist). Diffuse edema predominated in the spine (65.6%), whereas focal patterns were common in peripheral joints. Among infective, inflammatory, and neoplastic lesions (n = 48), diffusion restriction was observed in 56.3% and contrast enhancement in 83.3%. Final diagnoses included infective spondylodiscitis, trauma, degenerative arthritis, avascular necrosis, and neoplasia.

Conclusion: MRI is highly sensitive in detecting ELMSI and characterizing its patterns across musculoskeletal pathologies. Weight-bearing joints and the spine were most frequently affected. Advanced sequences such as DWI and post-contrast imaging added specificity in differentiating infective and malignant conditions. This is, to our knowledge, the first prospective multi-site study applying ELMSI terminology, supporting its adoption in routine radiological reporting

Keywords: *Bone marrow edema, edema-like marrow signal intensity, MRI, diffusion-weighted imaging, musculoskeletal radiology.*

How to Cite: Dr. Sanjay M. Khaladkar, Dr. Neeha Amit Jhala, Dr. Karishma Santosh Krishnani, Dr.Eshan Chetan Durgi, (2025) MRI-Based Characterization of Edema-Like Marrow Signal Intensity: A Prospective Case Series of 122 Patients, *Journal of Carcinogenesis*, *Vol.24, No.10s*, 205-214

1. INTRODUCTION

Edema-like marrow signal intensity (ELMSI), previously termed bone marrow edema (BME), is a nonspecific but clinically important finding on magnetic resonance imaging (MRI). It is defined as an area of low signal intensity on T1-weighted images and high signal on fluid-sensitive sequences such as T2-weighted fat-suppressed or short tau inversion recovery (STIR) images, reflecting an abnormal increase in marrow fluid content. Since the terminology "bone marrow edema" implied a histopathological diagnosis, the radiological descriptor "ELMSI" has been adopted to better represent the imaging appearance without presuming etiology [1].

ELMSI occurs in a wide spectrum of conditions, including trauma, degenerative joint disease, inflammatory and infective

arthropathies, ischemic disorders, neoplasia, and metabolic bone disease [2–4]. It may also be observed in transient, self-limiting entities such as migratory osteoporosis or bone marrow edema syndrome [5]. Although nonspecific, ELMSI correlates strongly with pain, functional limitation, accelerated joint degeneration, and increased risk of progression to arthroplasty in osteoarthritis [6,7].

MRI is the most sensitive modality for detection of ELMSI. Beyond simple visualization, advanced sequences such as diffusion-weighted imaging (DWI), chemical shift imaging, and dynamic contrast-enhanced MRI provide additional information to differentiate benign from malignant or infective etiologies [8,9]. However, interpretation remains challenging due to overlap in imaging appearances across conditions.

While several studies have described ELMSI in specific joints or diseases, few have comprehensively evaluated its distribution, imaging characteristics, and clinicopathological correlation across multiple anatomical sites within the same cohort. Understanding these patterns is essential for narrowing differential diagnoses, guiding biopsy, and informing clinical management.

The present prospective study was undertaken to evaluate ELMSI in a large cohort of patients using 3T MRI. Our objectives were to analyze its distribution across anatomical locations, identify predominant imaging patterns, assess the role of DWI and contrast enhancement in characterization, and correlate imaging findings with final clinicopathological diagnosis.

2. MATERIALS AND METHODS-

Study Design and Setting

This was a prospective, observational study conducted in the Department of Radiodiagnosis, Dr. D. Y. Patil Medical College, Hospital and Research Centre, Pune, between August 2022 and July 2024. The study was approved by the Institutional Ethics Committee. Written informed consent was obtained from all participants prior to inclusion.

Study Population

A total of 122 consecutive patients who underwent MRI for suspected marrow pathology were included. All age groups were eligible. Patients with infective, inflammatory, metabolic, neoplastic, iatrogenic, post-operative, and traumatic causes of marrow signal abnormalities were included.

Exclusion criteria were:

Physiological marrow changes, such as transient changes related to growth plate closure in children or sacroiliitis in postpartum women.

Mimics of marrow edema in the skull and unrelated conditions.

MRI Protocol

All examinations were performed on a 3 Tesla Siemens MAGNETOM Vida scanner. Patient positioning and coil selection varied with the anatomical site. The following sequences were obtained in axial, sagittal, and coronal planes:

T1-weighted imaging (T1WI)

T2-weighted imaging (T2WI)

Proton density fat-suppressed (PDFS)

Short tau inversion recovery (STIR)

Diffusion-weighted imaging (DWI) with apparent diffusion coefficient (ADC) mapping

Post-contrast T1-weighted fat-suppressed sequences (wherever clinically indicated)

Contrast was administered in cases with suspected infective, inflammatory, or neoplastic etiology.

Data Collection and Variables

For each patient, the following parameters were recorded:

Demographic data: age and sex

Anatomical location of ELMSI

Pattern of edema: focal or diffuse

Associated features: diffusion restriction on DWI, contrast enhancement, soft tissue changes

Final diagnosis based on clinical, radiological, pathological, and surgical correlation where available

Data Analysis

Data were entered into a master chart and analyzed using descriptive statistics. Frequencies and percentages were calculated for categorical variables, while means, ranges, and standard deviations were obtained for continuous variables. Observations were compared with final clinicopathological diagnoses to establish radiological-pathological correlation.

3. RESULTS-

A total of 122 patients with edema-like marrow signal intensity (ELMSI) were evaluated. The spine was the most frequently involved site (32 cases, 26.2%), followed by the knee (21 cases, 17.2%), ankle (17 cases, 13.9%), and hip (15 cases, 12.3%). The shoulder (14 cases, 11.5%), wrist (11 cases, 9.0%), and elbow (9 cases, 7.4%) were less commonly affected, while three cases (2.5%) involved other locations including the mandible, sacroiliac joint, and foot. Thus, weight-bearing regions accounted for the majority of cases.

The age of patients ranged from 12 to 87 years, with site-specific variation. The highest mean age was observed in the wrist (53.3 ± 18.6 years) and knee (53.1 ± 15.8 years), while the shoulder (39.3 ± 16.1 years), elbow (40.0 ± 20.5 years), and ankle (42.9 ± 16.6 years) were more commonly affected in younger or middle-aged groups. The spine (48.2 ± 19.4 years) and hip (44.3 ± 21.5 years) showed broader age ranges, reflecting their involvement across diverse etiologies.

Of the 122 patients, 66 were male (54.1%) and 56 female (45.9%). Male predominance was noted in the spine, shoulder, knee, and hip, while females predominated in ankle, wrist, and elbow involvement.

Regarding imaging patterns, focal edema was the predominant type (63.1%), especially in peripheral joints such as the ankle, knee, wrist, and elbow. In contrast, the spine showed a predominance of diffuse edema (65.6%), consistent with the higher proportion of infective and inflammatory pathologies in this region.

Advanced sequences added diagnostic value. Among patients with infective, inflammatory, or neoplastic etiologies (n = 48), diffusion restriction on DWI was observed in 56.3%. Restriction was most frequent in the elbow (100%) and spine (83.3%), followed by the knee (60%) and hip (50%). Similarly, contrast enhancement was present in 83.3% of such cases, predominantly in infective collections and malignant lesions. Enhancement patterns varied, with peripheral rim enhancement in abscesses, heterogeneous enhancement in malignancies, and synovial enhancement in inflammatory conditions.

Location-specific diagnostic patterns were observed. In the spine, infective spondylodiscitis (both pyogenic and tubercular) was most frequent, followed by spondylosis, fractures, and neoplasia. In the knee and wrist, traumatic and degenerative etiologies predominated, while in the ankle, diverse causes including osteochondritis dissecans, avascular necrosis, and rheumatoid arthritis were noted. The hip showed a higher frequency of avascular necrosis and neoplastic lesions. Across sites, final clinico-radiological-pathological correlation confirmed diagnoses in all cases.

Overall, this study demonstrated that ELMSI was most common in the spine and weight-bearing joints, with distinct site-specific age and sex distributions, edema patterns, and etiological associations. DWI and contrast-enhanced sequences provided additional specificity in characterizing infective and malignant cases.

4. DISCUSSION:

Magnetic resonance imaging (MRI) has revolutionized the evaluation of bone marrow abnormalities by enabling detection of subtle signal alterations that are not visible on plain radiography or computed tomography. The entity previously described as bone marrow edema (BME) is now more accurately termed edema-like marrow signal intensity (ELMSI) to emphasize that it is an imaging descriptor rather than a specific histopathological diagnosis [1]. In this study, we evaluated 122 consecutive patients with ELMSI, analyzing distribution across anatomical sites, age and sex variations, imaging patterns, and clinico-pathological correlation.

Distribution of ELMSI across anatomical sites

The present study demonstrated that the spine (26.2%) was the most common site of ELMSI, followed by the knee (17.2%), ankle (13.9%), and hip (12.3%). This distribution is consistent with prior reports that weight-bearing regions are particularly predisposed to marrow signal abnormalities because of their biomechanical stress [2,3]. In the spine, ELMSI was most frequently associated with infective spondylodiscitis, both pyogenic and tubercular, reflecting the endemic burden of spinal infections in the Indian subcontinent. These findings are in line with studies from tuberculosis-prevalent regions, which have highlighted marrow edema as a key early MRI feature of spinal infection [4].

Case 1 shows Pott's spine (Infective Spondylodiscitis), as in Fig. 1.

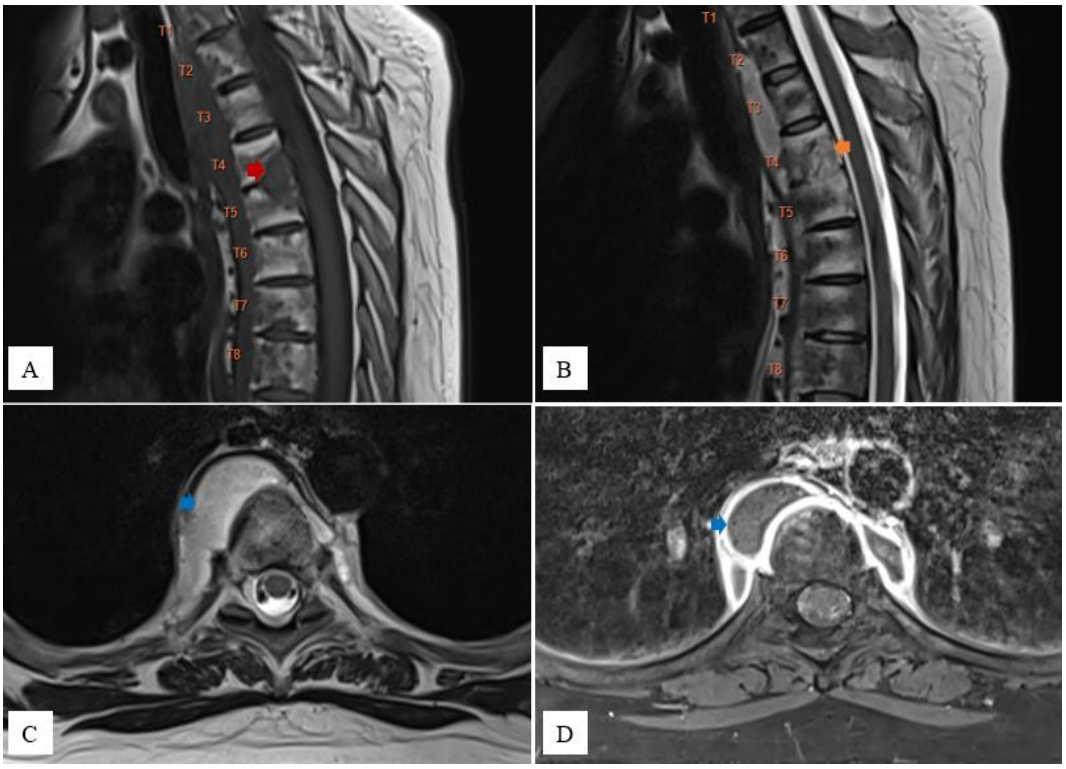

Figure 1: Bottom of Form

MRI of the thoracic spine, images A-D: A - T1-weighted sagittal image showing reduced disc space at the T4-T5 intervertebral disc levels with destruction of the adjacent vertebrae (red arrow). B - T2-weighted sagittal image demonstrating hyperintense ELMSI in the bodies of vertebrae T2-T8 (yellow arrow). C - T2-weighted axial image displaying hyperintense prevertebral and bilateral paravertebral soft tissue collections (blue arrow). D - T1-weighted post-contrast axial image revealing enhancement of the prevertebral and bilateral paravertebral soft tissue collections (blue arrow).

In the knee and wrist, traumatic etiologies predominated, consistent with the higher incidence of ligamentous and cartilaginous injuries in these joints. The ankle showed a broader spectrum, including osteochondritis dissecans, avascular necrosis, and rheumatoid arthritis, reflecting both mechanical and systemic causes. The hip demonstrated a higher frequency of avascular necrosis (AVN), consistent with its known vulnerability to vascular compromise [5]. Overall, these patterns underscore that while ELMSI is nonspecific, certain distributions may point toward characteristic underlying pathologies.

Age and sex distribution

In our cohort, the mean age varied by anatomical site. Knee (53.1 years) and wrist (53.3 years) involvement was more frequent in older individuals, consistent with degenerative osteoarthritis and osteonecrosis as primary etiologies. In contrast, shoulder, elbow, and ankle involvement was observed in younger and middle-aged patients, reflecting a higher contribution from trauma and overuse syndromes. Prior studies have similarly noted that degenerative marrow lesions increase with advancing age, while traumatic lesions occur across a wider age spectrum [6,7].

Case 2 shows Osteoarthritis (Degenerative disease), as in Fig. 2.

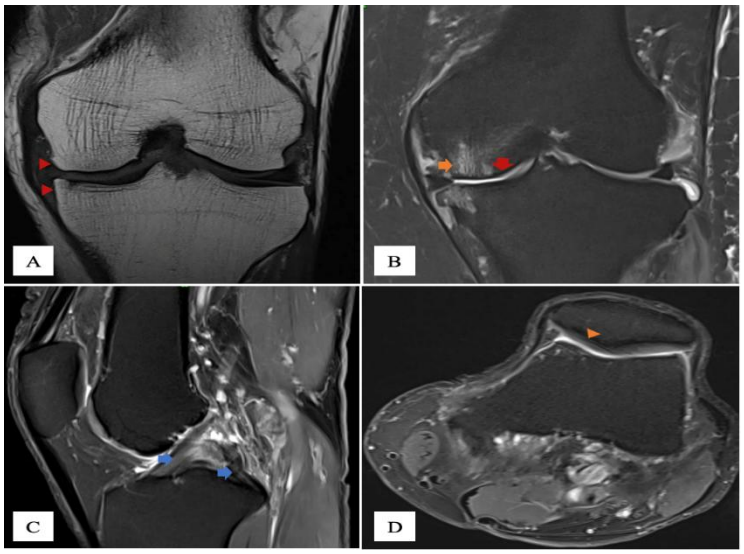

Figure 2: Bottom of Form

MRI left knee joint, images A-D: A - T1WI coronal image showing marginal osteophytes in the medial tibial and femoral condyles (red arrowheads). B - PDFS coronal image showing reduction in the medial tibiofemoral joint space with thinning of the articular cartilage (red arrow) and hyperintense ELMSI in the juxta-articular region of the medial tibial and femoral condyles (yellow arrow). C - PDFS sagittal image showing hyperintense signal in the anterior

Case 3 shows Sudeck's atrophy/ Complex regional pain syndrome (Trauma and overuse syndrome), as in Fig. 3.

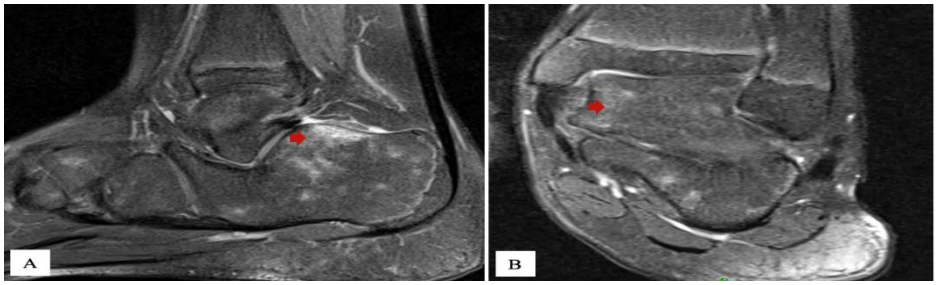

Figure 3: MRI right ankle, images A, B: A - PDFS sagittal image showing hyperintense ELMSI in the subcortical region of the calcaneum, talus, navicular, and cuboid bones (red arrow). B - PDFS coronal image depicting hyperintense ELMSI in the subcortical region of the calcaneum, talus, navicular, and cuboid bones (red arrow).

Case 4 shows Transient bone marrow edema syndrome (Trauma and overuse syndrome), as in Fig. 4.

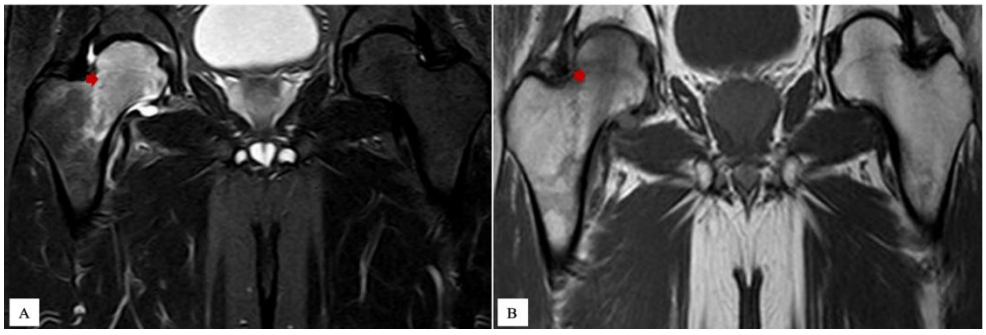

Figure 4: MRI bilateral hip joint, images A, B: A - STIR coronal image showing hyperintense ELMSI in the head and neck of the femur (red arrow). B - T1WI coronal image showing hypointense ELMSI (red arrow).

We observed a slight male predominance overall (54.1%), particularly in spine, shoulder, knee, and hip involvement. Females more frequently demonstrated ankle, elbow, and wrist ELMSI. This may relate to differing activity patterns, hormonal factors, and the higher prevalence of osteoporosis and rheumatoid arthritis among women [8].

Patterns of edema

In this study, focal edema predominated overall (63.1%), particularly in appendicular sites, while the spine showed a

predominance of diffuse edema (65.6%). Diffuse marrow involvement in the spine likely reflects infective and neoplastic etiologies, whereas focal lesions in peripheral joints are more often related to trauma or degenerative changes. Previous literature has emphasized that diffuse edema in the spine should raise suspicion for spondylodiscitis or metastasis, while focal, wedge-shaped subchondral edema is more typical of stress injuries and osteoarthritis [9,10].

Role of advanced MRI sequences

The addition of diffusion-weighted imaging (DWI) and contrast-enhanced imaging provided important diagnostic clues in our study. Diffusion restriction was observed in 56.3% of cases with infective, inflammatory, or neoplastic etiologies, particularly in spinal and elbow lesions. Restricted diffusion was seen in abscesses, soft tissue collections, and malignant tumors, while benign and degenerative lesions typically did not restrict. Prior studies have similarly demonstrated the value of DWI in differentiating infective spondylodiscitis from degenerative Modic changes and malignant from benign vertebral collapse [11,12]

Cases 5 and 6 show Ankylosing spondylitis, acute stage and Rheumatoid arthritis (Inflammatory diseases), as in Fig. 5, 6.

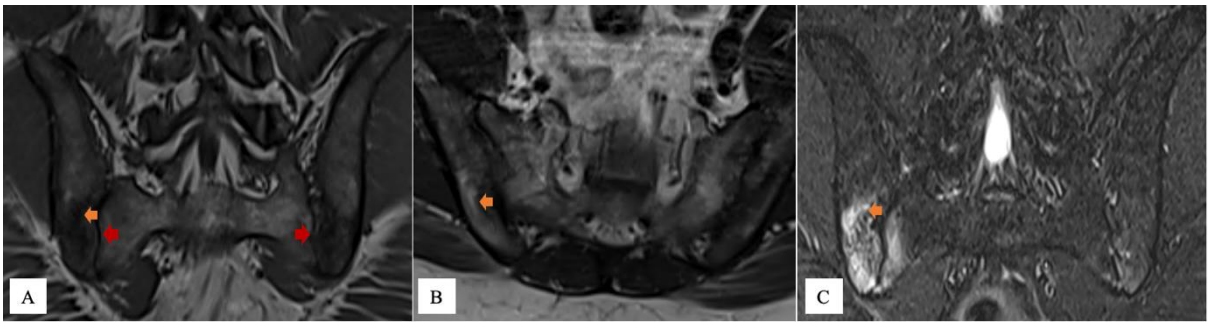

Figure 5: MRI sacroiliac joint screening, images A-C: T1WI coronal image showing narrowing of bilateral sacroiliac joints with erosion of adjacent articular surfaces (red arrows). Hypointense signal noted in the sacrum and right ilium depicting ELMSI (yellow arrow). B - T2 axial image showing hyperintense areas representing ELMSI (yellow arrow), in the sacrum and right ilium. C - STIR coronal image showing hyperintense ELMSI in the sacrum and right ilium (yellow arrow).

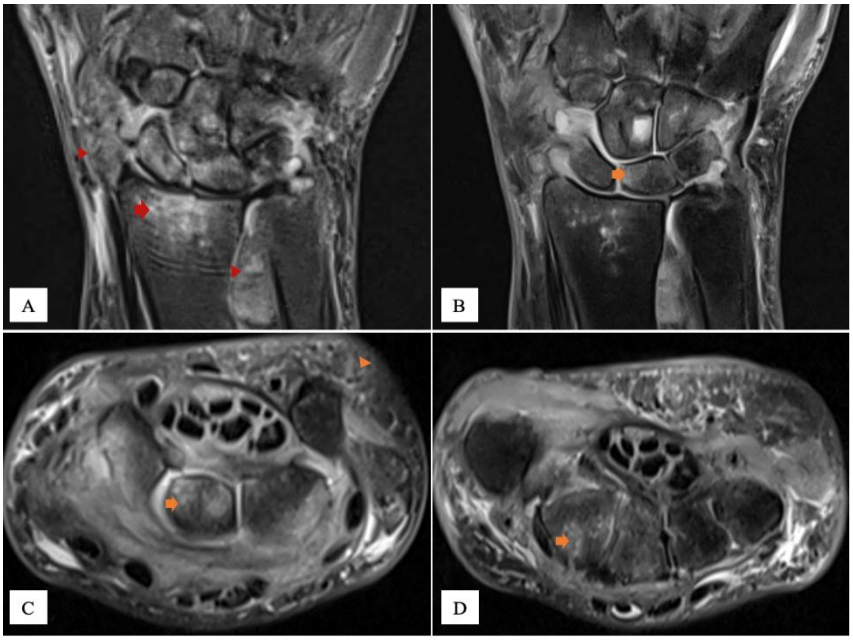

Figure 6: MRI right wrist joint, images A-D: A - PDFS coronal image depicting ELMSI in the distal end of the radius (red arrow) with synovial thickening in the distal radioulnar joint and the wrist joint (red arrowheads). B - PDFS image depicting narrowing of the intercarpal joint space, hyperintense ELMSI (yellow arrow), and effusion in the intercarpal joint space. C - PDFS axial image depicting hyperintense subcutaneous edema (yellow arrowhead), and hyperintense ELMSI in the carpal bones (yellow arrow). D - PDFS axial image showing hyperintense ELMSI in the 2nd and 3rd metacarpals.Contrast enhancement was present in 83.3% of infective, inflammatory, and neoplastic lesions in our cohort. Enhancement patterns were useful: peripheral rim enhancement in abscesses, heterogeneous enhancement in neoplasia, and synovial enhancement

in inflammatory arthropathies. Benign lesions rarely enhanced, except for vascular tumors and giant cell tumors. Similar observations have been reported by previous authors, who highlighted that enhancement pattern, rather than mere presence, is a key discriminator between benign, infective, and malignant processes [13].

Case 7 show Pott's spine and Septic arthritis (Infective disease), as in Fig. 7.

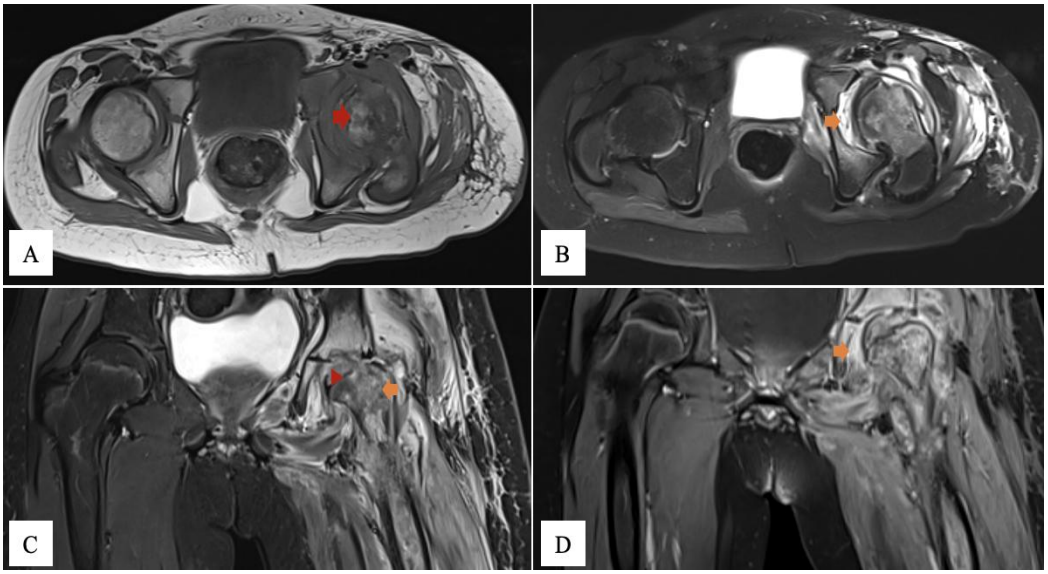

Figure 7: MRI bilateral hip, images A-D: A - T1WI axial image showing erosion of the left femoral head, appearing hypointense (red arrow). B - T2-weighted fat-suppressed axial image showing left hip joint effusion with synovial thickening (yellow arrow) and narrowing of the joint space. C - STIR coronal image showing flattening of the left femoral capital epiphysis (red arrowhead), ELMSI in the femoral head, greater trochanter, and shaft (blue arrow). Hyperintense intramuscular and subcutaneous edema is seen. D - T1WI post-contrast coronal image showing enhancement of the thickened synovium (yellow arrow).

Cases 8 and 9 show Giant cell tumor and Plasmacytoma (Neoplastic disease), as in Fig. 8, 9.

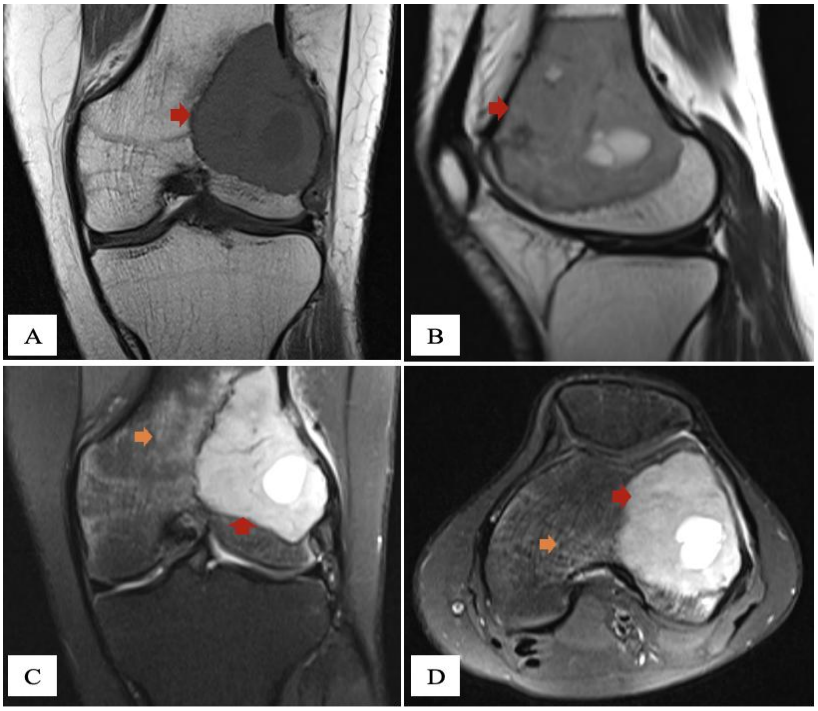

Figure 8: MRI Left knee joint, images A-D: A - T1WI coronal image showing an expansile lytic lesion at the epiphysiometaphyseal junction of the femur, appearing hypointense (red arrow). Fluid-fluid levels are visible within the lesion. B - T2WI sagittal image showing the same lesion (red arrow), appearing heterogeneously hyperintense with cystic areas within. C - PDFS coronal image and D - PDFS axial image showing the same lesion (red arrow), appearing hyperintense with surrounding ELMSI (yellow arrow).

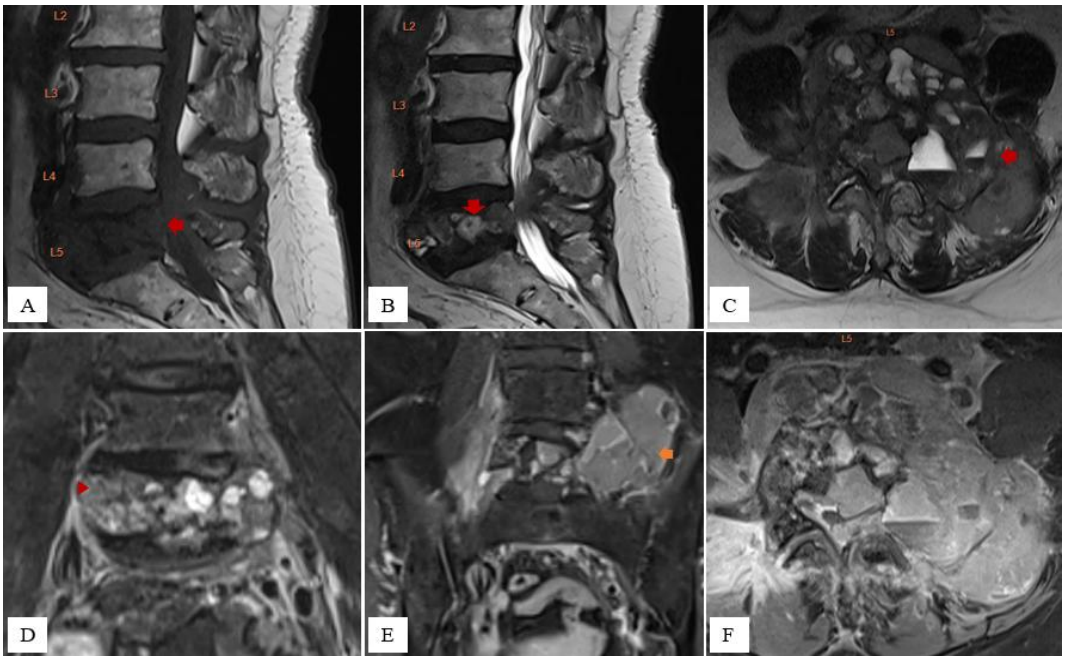

Figure 9: MRI of the lumbar spine, images A-F: A - T1-weighted sagittal image showing an expansile lytic lesion appearing hypointense in the body of the L5 vertebra (red arrow). B - T2-weighted sagittal image revealing a solid cystic lesion in the body of the L5 vertebra (red arrow). C - T2-weighted axial image displaying the same solid cystic lesion with fluid-fluid levels. The lesion extends into the posterior elements on the left side (red arrow). D, E - STIR coronal images showing hyperintense ELMSI in the L5 vertebra (red arrowhead). There is left paraspinal extension of the lesion causing compression of the left L5 exiting nerve roots (yellow arrow). F - T1-weighted post-contrast axial image depicting enhancement of the lesion

Correlation with final diagnoses

Radiological diagnosis correlated well with final clinicopathological outcomes in this study. In the spine, tuberculous and pyogenic spondylodiscitis were the leading causes of ELMSI, along with spondylosis and fractures. In the knee and wrist, traumatic injuries were predominant, while the hip showed higher prevalence of avascular necrosis and sarcomas. The ankle demonstrated diverse etiologies, including transient osteoporosis, osteochondritis dissecans, and inflammatory arthritis. These findings reinforce the fact that ELMSI is a common but heterogeneous manifestation across musculoskeletal diseases.

Clinical implications

Our findings carry several clinical implications. First, recognition of site-specific age and sex predilections may narrow the differential diagnosis when ELMSI is encountered. Second, careful analysis of pattern (focal vs diffuse), distribution (subchondral vs metaphyseal), and associated features improves specificity. Third, the use of DWI and contrast-enhanced sequences adds important discriminative power in infective and malignant conditions. Finally, correlation with clinical and laboratory parameters remains indispensable, since imaging alone cannot establish etiology in many cases.

Comparison with existing literature

The importance of ELMSI was first described in the late 1980s, when transient bone marrow edema syndrome of the hip and knee was recognized as a self-limiting disorder characterized by pain and spontaneous resolution [14]. Subsequent work established that marrow edema is a nonspecific marker of pathology that may arise from trauma, ischemia, infection, inflammation, or neoplasia [15,16]. Studies have highlighted its prognostic significance in osteoarthritis, where the presence and extent of marrow lesions predict cartilage loss, pain severity, and faster progression to arthroplasty [17,18].

MRI remains the modality of choice for detecting marrow edema, with fluid-sensitive sequences providing the highest sensitivity [19]. Advanced techniques such as chemical shift imaging and dynamic contrast-enhanced MRI have been shown to help differentiate benign marrow edema from tumor infiltration, while DWI improves confidence in characterizing spinal and pelvic lesions [20–22]. Recent work has also emphasized the value of semi-quantitative assessment of marrow edema volume in rheumatoid arthritis and osteoarthritis, correlating with disease activity and response to therapy [23,24].

Our results are consistent with these prior observations, while adding the strength of a comprehensive multi-site evaluation in a relatively large patient cohort. Importantly, we demonstrate that spinal and hip ELMSI in our population often reflects

infective and ischemic causes, whereas knee and wrist ELMSI is more often traumatic or degenerative. These variations highlight the need for contextual interpretation, particularly in regions with high prevalence of infections such as tuberculosis.

5. LIMITATIONS

This study has certain limitations. First, histopathological confirmation was not available in all cases; in some patients, the final diagnosis was based on clinicoradiological correlation and treatment response. Second, although a sample size of 122 is substantial, subgroup analysis by etiology at each site may require larger numbers for statistical power. Third, long-term follow-up to assess the prognostic implications of ELMSI was beyond the scope of this study. Despite these limitations, the prospective design, use of advanced MRI techniques, and comprehensive correlation with clinical outcomes strengthen the validity of our findings.

6. FUTURE DIRECTIONS

Future studies should focus on quantitative MRI biomarkers, including automated segmentation and volumetric assessment of marrow edema, to improve reproducibility and objectivity. The role of radiomics and artificial intelligence in distinguishing benign from malignant marrow signal changes warrants exploration. Additionally, longitudinal studies assessing the predictive value of ELMSI for outcomes such as joint replacement, fracture healing, and disease progression could further enhance clinical decision-making.

7. CONCLUSION-

Edema-like marrow signal intensity (ELMSI) is a frequent but nonspecific MRI finding encountered across a wide spectrum of musculoskeletal conditions. In this prospective study of 122 patients, the spine and weight-bearing joints emerged as the most common sites, with distribution and pattern varying according to age, sex, and underlying etiology. Diffuse edema was predominantly seen in spinal infections and neoplasms, while focal subchondral changes characterized traumatic and degenerative lesions in peripheral joints. Advanced MRI sequences, particularly diffusion-weighted imaging and contrast-enhanced studies, improved diagnostic confidence in differentiating infective and malignant conditions. Radiological interpretations correlated well with clinicopathological outcomes, underscoring the value of MRI as a first-line modality for marrow evaluation. Recognizing site-specific patterns and integrating imaging with clinical data are essential for accurate diagnosis and timely management. Future work incorporating quantitative and AI-driven MRI analysis may further enhance diagnostic precision and prognostic assessment

REFERENCES

[1] Gorbachova T, Amber I, Beckmann NM, Bennett DL, Chang EY, Davis L, et al. Nomenclature of subchondral nonneoplastic bone lesions. AJR Am J Roentgenol. 2019;213(5):963–72.

[2] Fernandez-Canton G, Casado O, Capelastegui A, Astigarraga E. Transient bone marrow oedema syndrome: findings in 9 cases. Eur Radiol. 1999;9(3):444–9.

[3] Wilson AJ, Murphy WA, Hardy DC, Totty WG. Transient osteoporosis: transient bone marrow edema? Radiology. 1988;167(3):757–60.

[4] Modic MT, Steinberg PM, Ross JS, Masaryk TJ, Carter JR. Degenerative disk disease: assessment of changes in vertebral body marrow with MR imaging. Radiology. 1988;166(1):193–9.

[5] Hofmann S, Engel A, Neuhold A, Leder K, Kramer J, Plenk H Jr. Bone-marrow oedema syndrome and transient osteoporosis of the hip. Clin Orthop Relat Res. 1993;(287):71–7.

[6] Felson DT, McLaughlin S, Goggins J, LaValley MP, Gale ME, Totterman S, et al. Bone marrow edema and its relation to progression of knee osteoarthritis. Ann Intern Med. 2003;139(5 Pt 1):330–6.

[7] Zanetti M, Bruder E, Romero J, Hodler J. Bone marrow edema pattern in osteoarthritic knees: correlation between MR imaging and histologic findings. Radiology. 2000;215(3):835–40.

[8] Hayes CW, Conway WF. Evaluation of articular and juxtaarticular marrow abnormalities with MR imaging. Radiology. 1992;183(1):193–9.

[9] Yao L, Lee JK, Rosenthal DI. MR imaging of bone marrow lesions of the knee: differential diagnosis. Radiology. 1987;164(2):731–5.

[10] Schweitzer ME, White LM. Does bone marrow edema represent trauma? AJR Am J Roentgenol. 1996;166(4):857–62.

[11] Baur A, Stäbler A, Arbogast S, Duerr HR, Bartl R, Reiser M. Diffusion-weighted MR imaging of bone marrow: differentiation of benign versus pathologic compression fractures. Radiology. 1998;207(2):349–56.

[12] Castillo M, Arbelaez A, Smith JK, Fisher LL. Diffusion-weighted MR imaging offers no advantage over

routine noncontrast MR imaging in the detection of vertebral metastases. AJNR Am J Neuroradiol. 2000;21(5):948–53.

[13] Vande Berg BC, Malghem J, Lecouvet FE, Maldague BE. Magnetic resonance imaging of normal bone marrow. Eur Radiol. 1998;8(8):1327–34.

[14] Radke S, Kenn W, Eulert J, Hahne HJ, Kalden JR, Stürmer KM. Transient bone marrow oedema of the hip: results of core decompression. Int Orthop. 1997;21(2):127–32.

[15] Zanetti M, Bruder E, Romero J, Hodler J. Bone marrow edema of the knee: histologic correlation and proposed diagnostic algorithm. Radiology. 2000;215(3):835–40.

[16] Hofmann S, Kramer J, Breitenseher M, Vecsei V. Bone marrow oedema syndrome and transient osteoporosis of the hip: an update. Semin Musculoskelet Radiol. 2001;5(1):59–71.

[17] Roemer FW, Neogi T, Nevitt MC, Felson DT, Zhu Y, Zhang Y, et al. Subchondral bone marrow lesions are highly associated with, and predict subchondral bone attrition longitudinally: the MOST study. Osteoarthritis Cartilage. 2010;18(1):47–53.

[18] Hunter DJ, Zhang Y, Niu J, Goggins J, Amin S, LaValley MP, et al. Increase in bone marrow lesions associated with cartilage loss: a longitudinal MRI study of knee osteoarthritis. Arthritis Rheum. 2006;54(5):1529–35.

[19] Vande Berg BC, Lecouvet FE, Malghem J, Maldague BE. Magnetic resonance imaging of normal and abnormal bone marrow. Eur Radiol. 1998;8(8):1327–34.

[20] Li X, Benjamin Ma C, Link TM. MR imaging of the ankle and foot: bone marrow edema pattern approach. Semin Musculoskelet Radiol. 2008;12(2):120–33.

[21] Vande Berg BC, Lecouvet FE, Malghem J. Magnetic resonance imaging of bone marrow lesions. Eur Radiol. 2000;10(12):2247–56.

[22] Lecouvet FE, Vande Berg BC, Maldague B, Malghem J. Magnetic resonance and radionuclide imaging in musculoskeletal disorders. Curr Opin Rheumatol. 2002;14(1):45–52.

[23] Li X, Kuo D, Schafer AL, Porzig A, Link TM, Majumdar S. Quantification of bone marrow edema-like lesions and subchondral cysts in knee osteoarthritis using MR imaging and a semi-automated segmentation method. Osteoarthritis Cartilage. 2010;18(9):1132–8.

[24] Ostergaard M, Peterfy C, Conaghan P, McQueen F, Bird P, Ejbjerg B, et al. OMERACT rheumatoid arthritis magnetic resonance imaging studies. Core set of MRI acquisitions, joint pathology definitions, and the OMERACT RA-MRI scoring system. J Rheumatol. 2003;30(6):1385–6..